PHYSICAL REVIEW D **81,** 037502 (2010)

Chiral random matrix model with 2 + 1 flavors at finite temperature and density

H. Fujii[1] and T. Sano[1,2]

[1]*Institute of Physics, University of Tokyo, Tokyo 153-8902, Japan*

[2]*Department of Physics, University of Tokyo, Tokyo 113-0033, Japan*

(Received 27 December 2009; published 10 February 2010)

Phase diagram of a chiral random matrix model with the two degenerate quarks (u and d) and the s-quark at finite temperature and density is presented. The model exhibits a first-order transition at finite temperature for three massless flavors, owing to the $U_A(1)$ breaking determinant term. We study the order of the transition with changing the quark masses and the quark chemical potential, and show that the first-order transition region expands as the chemical potential increases. We also discuss the behavior of the meson masses and the susceptibilities near the critical point.

DOI: 10.1103/PhysRevD.81.037502 PACS numbers: 25.75.Nq, 11.30.Qc, 11.30.Rd, 12.38.Lg

I. INTRODUCTION

Study of the QCD critical point (CP) [1–3] is an intriguing fundamental issue since its experimental confirmation will yield a strong evidence for the QCD phase transition, and energy-scan experiments searching for the QCD CP are being performed at the Relativistic Heavy Ion Collider at BNL. Although the existence of the critical point in the QCD phase diagram is presumably inferred from the model studies and lattice QCD results [1,2,4], its absence is also a possibility [4,5]. In this paper, we adopt as a schematic model for QCD the chiral random matrix (ChRM) model [6] which incorporates the $U_A(1)$-breaking determinant term [7,8]. We report the phase diagram of this model with the degenerate ud-quark mass $m_{\rm ud}$ and the s-quark mass $m_{\rm s}$ at finite temperature T and quark chemical potential μ.

The ChRM models have been successfully applied for qualitative study of chiral properties of QCD [9,10]. In a ChRM model the Dirac operator on gluon field background is modeled by a matrix D in the space of constant modes with small Dirac eigenvalues, retaining the chiral symmetry $\{D, \gamma_5\} = 0$. The partition function of the model is given as an average of $\det D$ over random ensemble of matrix elements, which mimics the complexity of the gluon dynamics. The finite T and μ effects are treated schematically as nonrandom external parameters appearing in D. In Ref. [10], the phase diagram of the ChRM model has been explored in the T-μ plane and a tricritical point (TCP) is found on the phase boundary in the massless limit. The TCP changes to a simple CP when the quark mass is nonzero. This result is consistent with the phase structure obtained in other model studies with two quark flavors [1,2,11] implying the scenario that the CP exists in the QCD phase diagram as an endpoint of the first-order phase boundary.

Nature of the chiral transition in QCD is sensitive to the number of light quark flavors, especially to the value of the s-quark mass $m_{\rm s}$. Unfortunately, however, the phase structure of the conventional ChRM model [10] is independent of the number of flavors N_f. In order to remedy this problem, we have recently incorporated the $U_A(1)$-breaking determinant interaction [7,8] in the ChRM model [6] by extending the zero-mode space [12] with the instanton gas model picture in mind. This is the first ChRM model which describes the N_f dependence of the chiral transition allowing us to explore the phase structure varying the parameters $m_{\rm ud}$ and $m_{\rm s}$ in addition to T and μ.

II. MODEL WITH DETERMINANT INTERACTION

The chiral symmetry breaking manifests itself in the nonzero density of the zero Dirac eigenvalues through the Banks-Casher relation [13]. The origin of small Dirac eigenvalues may be instanton configurations of background gauge field and other nonperturbative gluon dynamics. Here in our model we divide these fermionic modes into two categories, N_+ and N_- topological zero modes associated with N_+ instantons and N_- anti-instantons, respectively, and $2N$ near-zero modes generated by other complex dynamics [6,12]. The Dirac operator D then approximated with a matrix of $2N + N_+ + N_-$ dimensions with N_+, N_- and N being of the order of the space-time volume $\mathcal{O}(V)$. The thermodynamic limit is taken as $2N + N_+ + N_- \to \infty$. Note that $N_\pm$ should vary depending on the instanton distribution.

For fixed number of zero modes the model partition function is written in the chiral basis as

$$Z_{N_+,N_-} = \int dR \mathrm{e}^{-N\Sigma^2 \mathrm{tr} RR^\dagger} \prod_{f=1}^{N_f} \det(D + m_f), \qquad (1)$$

with

$$D = \begin{pmatrix} 0 & \mathrm{i}R + C \\ \mathrm{i}R^\dagger + C^T & 0 \end{pmatrix}, \qquad (2)$$

where $R \in \mathbb{C}^{(N+N_+)\times(N+N_-)}$ is a random matrix following a Gaussian ensemble distribution with the variance $1/(N\Sigma^2)$ and $C \in \mathbb{C}^{(N+N_+)\times(N+N_-)}$ is a matrix representing the effects of T and μ. The matrix D has $|N_+ - N_-|$ exact zero eigenvalues when R and C are rectangular, which is interpreted as a realization of the index theorem in the ChRM model. We adopt here the simplest form for C [10]:

$$C = \begin{pmatrix} (\mu + iT)\mathbf{1}_{N/2} & 0 & 0 \\ 0 & (\mu - iT)\mathbf{1}_{N/2} & 0 \\ 0 & 0 & 0 \end{pmatrix}, \quad (3)$$

where T and μ are schematic representation for the temperature and chemical potential effects, respectively. Note that D with $\mu \neq 0$ is non-Hermitian, whereas the partition function (1) is still invariant under $\mu \leftrightarrow -\mu$. One should appreciate that the $N_+ \times N_-$ right-bottom block in C corresponding to the topological zero modes is set to zero. This seems a reasonable assumption if one notices that the finite T and μ effects are introduced as a boundary condition in the Matsubara formalism and that the localized topological zero modes will be insensitive to the boundary. This discrimination is important indeed in reproducing the physical T dependence of the topological susceptibility [6,14].

The complete partition function of the model is obtained by summing over N_+ and N_- with a distribution $P(N_\pm)$:

$$Z^{\mathrm{RM}} = \sum_{N_+,N_-} P(N_+)P(N_-)Z_{N_+,N_-}. \quad (4)$$

The $P(N_\pm)$ reflects a modeling of the instanton distribution in the QCD ground state. The authors of Ref. [12] adopted the Poisson distribution, which involves arbitrarily large number for $N_\pm$ and results in a model with no stable ground state. Inspired by the lattice gas model within a finite box, we instead choose the binomial distribution [6],

$$P(N_\pm) = \binom{\gamma N}{N_\pm} p^{N_\pm}(1-p)^{\gamma N - N_\pm}, \quad (5)$$

where γ is a parameter of $\mathcal{O}(V^0)$ and p is interpreted as the probability for a single instanton to occupy a unit volume $V/(\gamma N)$. This distribution sets an upper bound γN for $N_\pm$ and gives rise to a stable effective potential as a function of order parameters. In fact, applying the standard bosonization procedure to (4), we find

$$\begin{aligned} Z^{\mathrm{RM}} &= \int dS \mathrm{e}^{-N\Sigma^2 \mathrm{tr} S^\dagger S} \\ &\quad \times \det{}^{N/2}[(S+\mathcal{M})(S^\dagger+\mathcal{M}^\dagger) - (\mu+iT)^2] \\ &\quad \times \det{}^{N/2}[(S+\mathcal{M})(S^\dagger+\mathcal{M}^\dagger) - (\mu-iT)^2] \\ &\quad \times [\alpha \det(S+\mathcal{M}) + 1]^{\gamma N}[\alpha \det(S^\dagger+\mathcal{M}^\dagger) + 1]^{\gamma N} \\ &\equiv \int dS \mathrm{e}^{-2N\Omega(S;T,\mu)}, \end{aligned} \quad (6)$$

where we defined the effective potential $\Omega(S; T, \mu)$ in the last line. $S \in \mathbb{C}^{N_f \times N_f}$ is the order parameter matrix, and $\mathcal{M}$ is the mass matrix. The parameter $\alpha = p/(1-p)$. Note that the integrand of Z^{RM} is a polynomial of S except for the exponential factor originating from the Gaussian ensemble distribution. Large values of S are suppressed by this Gaussian weight.

The determinant term with the coefficient α represents the anomaly which breaks explicitly the $\mathrm{U}_A(1)$ symmetry of $\Omega(S)$. For $S = \phi \mathbf{1}_{N_f}$ ($\phi \in \mathbb{R}$) with $\mathcal{M} = 0$, Ω simplifies to

$$\Omega_{N_f} = \frac{N_f}{2}\left(\Sigma^2\phi^2 - \frac{1}{2}\ln[\phi^2 - (\mu+iT)^2] \times [\phi^2 - (\mu-iT)^2]\right) - \gamma \ln|\alpha\phi^{N_f} + 1|. \quad (7)$$

We see that the anomaly term yields $-\alpha\gamma\phi^{N_f}$ when expanded. In Ref. [6] we studied this ChRM model with two and three equal-mass flavors at finite T with $\mu = 0$, to show a second- (first-) order phase transition for $N_f = 2(3)$.

III. PHASE DIAGRAM AND MESON MASSES WITH 2 + 1 FLAVORS

Choosing $S = \mathrm{diag}(\phi_{\mathrm{ud}}, \phi_{\mathrm{ud}}, \phi_{\mathrm{s}})$ in the $2+1$ flavor case with $\mathcal{M} = \mathrm{diag}(m_{\mathrm{ud}}, m_{\mathrm{ud}}, m_{\mathrm{s}})$, we have

$$\begin{aligned} \Omega &= \Sigma^2\phi_{\mathrm{ud}}^2 - \tfrac{1}{2}(\ln[\varphi_{\mathrm{ud}}^2 - (\mu+iT)^2] + (T \to -T)) \\ &\quad + \tfrac{1}{2}\Big[\Sigma^2\phi_{\mathrm{s}}^2 - \tfrac{1}{2}(\ln[\varphi_{\mathrm{s}}^2 - (\mu+iT)^2] + (T \to -T))\Big] \\ &\quad - \gamma \ln|\alpha\varphi_{\mathrm{ud}}^2\varphi_{\mathrm{s}} + 1|, \end{aligned} \quad (8)$$

where $\varphi_{\mathrm{ud}} = \phi_{\mathrm{ud}} + m_{\mathrm{ud}}$ and $\varphi_{\mathrm{s}} = \phi_{\mathrm{s}} + m_{\mathrm{s}}$. The ground state is determined by the saddle-point condition

$$\frac{\partial\Omega}{\partial\phi_{\mathrm{ud}}} = 0, \qquad \frac{\partial\Omega}{\partial\phi_{\mathrm{s}}} = 0, \quad (9)$$

which becomes exact in the thermodynamic limit.

Prior to the numerical analysis, we comment on the model parameters Σ, α, and γ. Setting $\Sigma = 1$ by redefinition of S and other parameters, we searched such a set of parameters α, γ, m_{ud}, and m_{s}, which reproduces quantitatively the (ratios of the) meson masses in the vacuum, but it was unsuccessful. However, the model can describe the mass hierarchy qualitatively as seen below in Fig. 3, and we wish to study the model phase diagram as an schematic model for QCD. Note that all the quantities are dimensionless in this work.

We also remark that the anomaly term makes a symmetry-broken phase more stable. Indeed, no symmetry restoration occurs at finite T for $\alpha\gamma > \Sigma^2(=1)$ with $N_f = 2$, and the situation is similar even for $N_f = 3$. Hence, one must assume $\alpha\gamma \lesssim 1$ for study of the chiral restoration.

Finally, the transition at finite $\mu \neq 0$ with $T = 0$ is first-order. It is seen in the simple case (7) because the symmetric phase $\phi = 0$ and the broken phase $\phi > \mu$ are separated with the point $\phi = \mu$ where $\Omega = \infty$ or the integrand of Z^{RM} vanishes. This feature survives in more general cases with $2+1$ flavors.

Let us study the phase diagram in the T-m_{ud}-m_{s} space. Since our model shows a first-order transition at finite T for $m_{\mathrm{ud}} = m_{\mathrm{s}} = 0$ and a crossover for large m_{ud} and m_{s} [6], there must be a line of a second-order transition separating these two regions in the m_{ud}-m_{s} plane. This critical line is determined by the condition $\Omega^{(n)} = 0$ ($n = 1, 2, 3$) with $\Omega^{(n)} \equiv \partial^n\Omega/\partial\phi_{\mathrm{ud}}^n$, where Ω is a function of a single order parameter ϕ_{ud} with ϕ_{s} eliminated by the second equation

in (9). Note that $\Omega^{(2)} = 0$ is equivalent to $\det[\partial^2\Omega(S)/\partial\phi_i\partial\phi_j] = 0$ $(i,\ j = \mathrm{ud},\ \mathrm{s})$, which implies the vanishing σ mass (see below).

We present in Fig. 1 the critical line projected on the m_{ud}-m_{s} plane for several values of α and γ. When we increase the strength of the anomaly term α and/or γ, the region of the first-order transition expands. For each parameter a TCP is found on the m_{s} axis, where the $N_f = 2$ chiral transition changes from a first to a second-order one. Near the TCP the critical line behaves as $(m_{\mathrm{s}}^{\mathrm{TCP}} - m_{\mathrm{s}}) \propto m_{\mathrm{ud}}^{2/5}$ as is expected from the Landau-Ginzburg analysis, which is clearly seen in Fig. 1(b). On the other hand, the line smoothly intersects the m_{ud} axis with a finite slope. In fact, the model with the anomaly term is symmetric under $m_{\mathrm{ud}} \leftrightarrow -m_{\mathrm{ud}}$ but asymmetric under $m_{\mathrm{s}} \leftrightarrow -m_{\mathrm{s}}$.

Next we extend our calculation to the finite μ case. Figure 2 exhibits the phase diagram in the m_{ud}-m_{s}-μ^2 space. We see that the region of the first-order transition expands as μ is increased. This behavior indicates the existence of the CP in the T-μ plane with the physical quark masses, provided that the finite-T transition at $\mu = 0$ is crossover. Varying the anomaly parameters α and γ, we have confirmed that the expansion of the first-order region with increasing μ is a robust result in our model as far as we keep α and γ constant.

The (screening) mass matrices for the scalar and pseudoscalar mesons are defined as the curvature of the potential around $\bar{S} = \mathrm{diag}(\phi_{\mathrm{ud}}, \phi_{\mathrm{ud}}, \phi_{\mathrm{s}})$:

$$M^{\mathrm{s2}}_{ab} = \frac{\partial^2\Omega(S)}{\partial\sigma_a\partial\sigma_b}\bigg|_{S=\bar{S}}, \qquad M^{\mathrm{ps2}}_{ab} = \frac{\partial^2\Omega(S)}{\partial\pi_a\partial\pi_b}\bigg|_{S=\bar{S}}, \quad (10)$$

where $S = \lambda_a(\sigma_a + \mathrm{i}\pi_a)/\sqrt{2}$ with real parameters σ_a and π_a, and with λ_a being the Gell-Mann matrices and $\lambda_0 = \sqrt{\frac{2}{3}}\mathrm{diag}(1, 1, 1)$. See the Appendix for explicit expressions for M^2_{ab}. Because the SU(3) flavor symmetry is broken by $m_{\mathrm{ud}} \neq m_{\mathrm{s}}$, there are nonzero mixing $M^2_{08} = M^2_{80} \neq 0$ and the mass eigenvalues σ and f_0 for the scalars and η and η' for the pseudoscalars are obtained after diagonalization. One can show that the flat direction of $\Omega(\phi_{\mathrm{ud}}, \phi_{\mathrm{s}})$ near the CP coincides with the σ fluctuation direction.

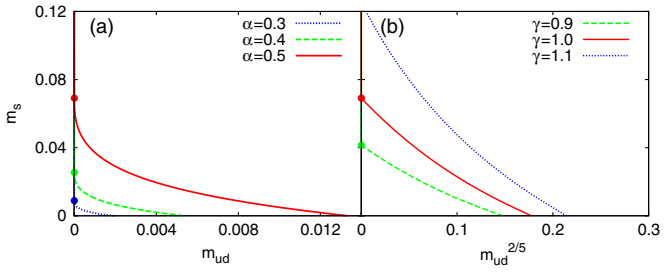

FIG. 1 (color online). The critical curves on the m_{ud}-m_{s} plane (a) for $\alpha = 0.3, 0.4, 0.5$ with $\gamma = 1$ and (b) for $\gamma = 0.9, 1.0, 1.1$ with $\alpha = 0.5$. The finite-T transition is first order in the smaller-mass region and crossover in the larger-mass region. On the m_{s} axis with $m_{\mathrm{ud}} = 0$, there is the $N_f = 2$ chiral symmetry. The TCP is denoted by a dot for each parameter.

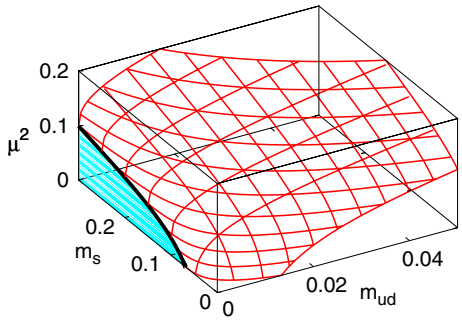

FIG. 2 (color online). Critical surface in the m_{ud}-m_{s}-μ^2 space with the parameters $\gamma = 1$ and $\alpha = 0.5$. A series of TCP's is denoted by a thick line, and the second-order transition with $N_f = 2$ chiral symmetry occurs in the shaded area.

In Fig. 3, we show the meson masses as a function of μ at $T = T_c$ with parameters $\gamma = 1$, $\alpha = 0.5$, $m_{\mathrm{ud}} = 0.05$ and $m_{\mathrm{s}} = 1.0$. The model reproduces the empirical hierarchy of the meson masses qualitatively in small μ region, thanks to the anomaly term. With increasing T and/or μ the pseudoscalar meson masses remain nearly constant while the scalar ones, especially the σ mass, decrease. At the CP $(T = T_c,\ \mu = \mu_c)$, the σ meson becomes massless. At higher $\mu > \mu_c$, pairs of the masses M_σ-M_π, M_κ-M_K, and M_δ-$M_{\eta'}$ get almost degenerate, reflecting the approximate $N_f = 2$ chiral symmetry.

Generalizing the mass matrix to $\mathcal{M} = \lambda_a(s_a + \mathrm{i}p_a)/\sqrt{2}$ with real sources s_a and p_a, the scalar susceptibilities are defined as

$$\chi^{\mathrm{s}}_{ab} = -\frac{\partial^2\Omega(S(\mathcal{M});\mathcal{M})}{\partial s_a\partial s_b}, \quad (11)$$

where $S(\mathcal{M})$ solves (9) for a fixed $\mathcal{M}$, and the derivatives are evaluated at $\mathcal{M} = \mathrm{diag}(m_{\mathrm{ud}}, m_{\mathrm{ud}}, m_{\mathrm{s}})$. The pseudoscalar susceptibilities χ^{ps}_{ab} are defined similarly as the response to p_a. We find the (pseudo-)scalar susceptibilities $\chi^{\mathrm{s(ps)}}_{ab}$ in a diagonal form

$$\chi^{\mathrm{s(ps)}}_{ab} = \delta_{ab}\Sigma^2(\Sigma^2/M^{\mathrm{s(ps)2}}_{aa} - 1) \quad (12)$$

for $a, b = 1, \ldots, 7$. There is an mixing term for $a, b = 0, 8$

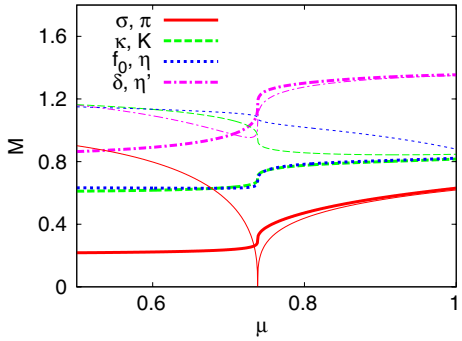

FIG. 3 (color online). Mesonic masses as functions of μ with $T = T_c$ fixed for parameters $\gamma = 1$, $\alpha = 0.5$, $m_{\mathrm{ud}} = 0.05$, and $m_{\mathrm{s}} = 1.0$. The critical point locates at $(T_c, \mu_c) = (0.817, 0.738)$. Thin (thick) lines indicate (pseudo-)scalar mesons.

due to the SU(3) breaking:

$$\chi^{\mathrm{s(ps)}}_{ab} = \Sigma^2(\Sigma^2(M^{\mathrm{s(ps)2}})^{-1}_{ab} - \delta_{ab}), \tag{13}$$

which becomes diagonal when the mass matrix $M^{\mathrm{s(ps)2}}$ is transformed to be diagonal. Note that the scalar susceptibility in the σ channel diverges when the (screening) mass M_σ vanishes at the CP. So do the quark number susceptibility $\chi_q = -\partial^2\Omega/\partial\mu^2$ as well as the "specific heat" $\chi_T = -\partial^2\Omega/\partial T^2$, through the mode mixing generated by the finite condensate φ_{ud} and φ_{s} [15].

IV. CONCLUSION

As a schematic model for QCD, we have analyzed for the first time in the ChRM model the phase structure with $2 + 1$ flavors at finite T and μ, which becomes possible by the inclusion of the $\mathrm{U}_A(1)$ breaking term [6]. We have drawn the critical curve separating the first-order transition region and the crossover region in the m_{ud}-m_{s} plane with $\mu = 0$, and we have shown that the first-order transition region expands as the strength of the anomaly term is increased.

Extending the model to the finite μ case, we have shown the critical surface in the m_{ud}-m_{s}-μ space. We have found that the first-order transition region expands with increasing μ, which is a supportive result for the existence of QCD CP on the T-μ plane: one encounters a CP as μ is increased from zero, provided that the finite-T transition is crossover at $\mu = 0$. The meson mass hierarchy in the vacuum is qualitatively reproduced with the $\mathrm{U}_A(1)$ anomaly term and the SU(3) flavor breaking. At the CP the (screening) mass of σ vanishes. Although we treat the model parameters independent of T and μ, possible rapid quenching of these parameters at finite μ can give rise to a shrinkage of the first-order transition region [16]. Furthermore, the role of the vector interaction between the quarks [17] deserves further study. These are beyond the scope of this schematic model.

APPENDIX

The mass matrix M^2_{ab} is diagonal except for $a, b = 0$ and 8. For $a = 1, 2, 3$ and for $a = 4, \ldots, 7$, respectively,

$$M^2_{\delta,\pi} = \Sigma^2 \pm \mathrm{Re}\frac{\varphi^2_{\mathrm{ud}} \pm z^2}{(\varphi^2_{\mathrm{ud}} - z^2)^2} \pm \gamma\frac{\alpha\varphi_{\mathrm{s}}}{\alpha\varphi^2_{\mathrm{ud}}\varphi_s + 1}, \tag{A1}$$

$$M^2_{\kappa,K} = \Sigma^2 \pm \mathrm{Re}\frac{\varphi_{\mathrm{ud}}\varphi_{\mathrm{s}} \pm z^2}{(\varphi^2_{\mathrm{ud}} - z^2)(\varphi^2_{\mathrm{s}} - z^2)} \pm \gamma\frac{\alpha\varphi_{\mathrm{ud}}}{\alpha\varphi^2_{\mathrm{ud}}\varphi_s + 1}, \tag{A2}$$

where $z = \mu + \mathrm{i}T$. The upper (lower) sign corresponds to the (pseudo-) scalar meson. The elements M^2_{ab} for $a, b = 0, 8$ are written concisely in another basis of $\lambda_{\mathrm{ud}} \equiv \mathrm{diag}(1, 1, 0)$ and $\lambda_{\mathrm{s}} \equiv \mathrm{diag}(0, 0, \sqrt{2})$, instead of $\lambda_{0,8}$:

$$M^2_{\mathrm{ud,ud}} = \Sigma^2 \pm \mathrm{Re}\frac{\varphi^2_{\mathrm{ud}} \pm z^2}{(\varphi^2_{\mathrm{ud}} - z^2)^2} \pm \gamma\frac{\alpha^2\varphi^2_{\mathrm{ud}}\varphi^2_{\mathrm{s}} - \alpha\varphi_{\mathrm{s}}}{(\alpha\varphi^2_{\mathrm{ud}}\varphi_{\mathrm{s}} + 1)^2}, \tag{A3}$$

$$M^2_{\mathrm{s,s}} = \Sigma^2 \pm \mathrm{Re}\frac{\varphi^2_{\mathrm{s}} \pm z^2}{(\varphi^2_{\mathrm{s}} - z^2)^2} \pm \gamma\frac{\alpha^2\varphi^4_{\mathrm{ud}}}{(\alpha\varphi^2_{\mathrm{ud}}\varphi_{\mathrm{s}} + 1)^2}, \tag{A4}$$

$$M^2_{\mathrm{ud,s}} = M^2_{\mathrm{s,ud}} = \mp\sqrt{2}\gamma\frac{\alpha\varphi_{\mathrm{ud}}}{(\alpha\varphi^2_{\mathrm{ud}}\varphi_{\mathrm{s}} + 1)^2}. \tag{A5}$$

[1] M. Asakawa and K. Yazaki, Nucl. Phys. **A504**, 668 (1989).
[2] A. Barducci *et al.*, Phys. Lett. B **231**, 463 (1989).
[3] For review, M. Stephanov, Prog. Theor. Phys. Suppl. **153**, 139 (2004); Proc. Sci., LAT2006 (2007) 024.
[4] For review, E. Laermann and O. Philipsen, Annu. Rev. Nucl. Part. Sci. **53**, 163 (2003); O. Philipsen, Prog. Theor. Phys. Suppl. **174**, 206 (2008); P. de Forcrand, Proc. Sci., LAT2009 (2009) 010.
[5] P. de Forcrand and O. Philipsen, J. High Energy Phys. 01 (2007) 077.
[6] T. Sano, H. Fujii, and M. Ohtani, Phys. Rev. D **80**, 034007 (2009).
[7] M. Kobayashi and T. Maskawa, Prog. Theor. Phys. **44**, 1422 (1970); M. Kobayashi, H. Kondo, and T. Maskawa, Prog. Theor. Phys. **45**, 1955 (1971).
[8] G. 't Hooft, Phys. Rev. Lett. **37**, 8 (1976); Phys. Rev. D **14**, 3432 (1976); **18**, 2199(E) (1978).
[9] E. V. Shuryak and J. J. M. Verbaarschot, Nucl. Phys. **A560**, 306 (1993); A. D. Jackson and J. J. M. Verbaarschot, Phys. Rev. D **53**, 7223 (1996); T. Wettig, A. Schäfer, and H. A. Weidenmüller, Phys. Lett. B **367**, 28 (1996); **374**, 362(E) (1996); M. A. Stephanov, Phys. Rev. Lett. **76**, 4472 (1996); For review, J. J. M. Verbaarschot and T. Wettig, Annu. Rev. Nucl. Part. Sci. **50**, 343 (2000).
[10] A. M. Halasz *et al.*, Phys. Rev. D **58**, 096007 (1998).
[11] J. Berges and K. Rajagopal, Nucl. Phys. **B538**, 215 (1999).
[12] R. A. Janik, M. A. Nowak, and I. Zahed, Phys. Lett. B **392**, 155 (1997).
[13] T. Banks and A. Casher, Nucl. Phys. **B169**, 103 (1980).
[14] M. Ohtani *et al.*, Mod. Phys. Lett. A **23**, 2465 (2008); C. Lehner *et al.*, Phys. Rev. D **79**, 074016 (2009).
[15] Y. Hatta and T. Ikeda, Phys. Rev. D **67**, 014028 (2003); H. Fujii, Phys. Rev. D **67**, 094018 (2003); H. Fujii and M. Ohtani, Phys. Rev. D **70**, 014016 (2004).
[16] K. Fukushima, Phys. Rev. D **77**, 114028 (2008); **78**, 039902(E) (2008); J. W. Chen *et al.*, Phys. Rev. D **80**, 054012 (2009); B. J. Schaefer and M. Wagner, Phys. Rev. D **79**, 014018 (2009).
[17] M. Kitazawa *et al.*, Prog. Theor. Phys. **108**, 929 (2002); Y. Sakai *et al.*, Phys. Rev. D **78**, 076007 (2008); K. Fukushima, Phys. Rev. D **78**, 114019 (2008).